Reprint

J.M. Costa, A.N. Venetsanopoulos and M. Trefler, "Evaluation of digital tomographic filters", *IEEE Transactions on Medical Imaging*, Vol. MI-4, No. 1, pp. 1-13, March 1985.

Evaluation of Digital Tomographic Filters

JOSÉ M. COSTA, ANASTASIOS N. VENETSANOPOULOS, AND MARTIN TREFLER

Abstract—Recently, a technique has been proposed to filter conventional radiographs in order to obtain depth-dependent information by simulating standard tomography. This technique has been referred to as tomographic filtering or tomographic filtration process (TFP). It takes advantage of the finite size of the X-ray source, so that after processing the image of a particular layer is improved, while the others are degraded. This paper briefly reviews this technique and then concentrates on its analytical evaluation. A comparative assessment of tomographic filtering is produced taking as benchmarks two well established radiologic procedures: standard tomography and conventional radiology. The comparison is made on the basis of the following evaluation criteria: the exposure angle, the thickness of the cut, the rate of change of the transfer function, the signal-to-noise ratio, and the radiation dose. Practical evaluations are also shown.

I. Introduction

RECENTLY, a technique has been proposed to filter conventional radiographs in order to obtain depth-dependent information by simulating standard tomography [1]-[3]. This technique takes advantage of the finite size of the X-ray source, so that after processing, the image of a particular layer is improved while the others are degraded. This technique has been referred to as tomographic filtering or tomographic filtration process (TFP) [1]-[3]. The second term usually denotes not only the filter, but also the X-ray system, that is, the complete system. The objective of this paper is to give an analytical evaluation of tomographic filtering. A summary of this evaluation has appeared in [1], [3].

Tomographic filtering is reviewed in Section II. A comparative assessment of tomographic filtering is produced in Section III, taking as benchmarks two well established radiologic procedures: standard tomography and conventional radiology. Section IV discusses some practical evaluations, and results with actual radiographs are shown to support this theory. The conclusions in Section V indicate that the main advantage of tomographic filtering is in reducing the total radiation dose to the patient.

II. Tomographic Filters

Tomographic filtering uses the depth-dependent focal-spot blur and will be understood better by comparing it with standard tomography.

Standard tomographic techniques produce a tomogram by moving a point-like X-ray source and the recording film in a coupled manner, so that during the exposure only the parts of the body lying in one specific plane parallel to the film plane are always projected on the same place on the film, while the others are blurred. The layer whose image is in focus is referred to as the plane of cut or tomographic layer.

A tomographic filtration process (TFP) should produce a focusing effect similar to that of standard tomography, but with no moving parts. In a TFP, instead of moving the X-ray tube, the finite size of the focal spot is used to advantage and instead of moving the film, a filter is used to process a conventional radiograph. Indeed, by applying superposition we can imagine an equivalent source of X-rays by moving a hypothetical point source over the region of the actual source. The movement of this point source is analogous to the movement of an X-ray tube in standard tomography. Since in conventional radiography the film does not move, the images of all the layers are blurred. Therefore, in order to convert a radiograph into a tomogram the radiographic image is processed by a filter that will produce an effect equivalent to that produced by the motion of the film in standard tomography.

To illustrate this phenomenon consider the diagram in Fig. 1. Suppose that the tomographic layer is at a distance Δ_1 from the focal spot s and at a distance Δ_2 from the film plane. If 0 is a point on the tomographic layer, its image on the film extends over a distance U as shown in Fig. 1. This blur U is the one that we want to eliminate. Here we define blur as the extent of the image of a point or edge due to the finite size of the focal spot. All other blurs corresponding to other layers, such as the blur V of the point X and the blur V' of the point X', differ in size and therefore cannot be eliminated simultaneously. The extension to two dimensions is straightforward.

The equations of tomographic filtering have been derived in detail [1]. The results showed that the equations of image formation in standard tomography, conventional radiology, and tomographic filtering are similar.[1]

The frequency-domain equation of image formation in radiology is

$$G(f_x, f_y) = I_B \delta(f_x, f_y) - \int_0^d H_i(f_x, f_y, z_i)\, F_\mu(f_x, f_y, z_i)\, dz_i \qquad (1)$$

where $G(f_x, f_y)$ is the Fourier transform of the resulting

Manuscript received February 6, 1984; revised December 3, 1984.

J. M. Costa is with Bell-Northern Research, Ottawa, Ont., Canada K1Y 4H7.

A. N. Venetsanopoulos is with the Department of Electrical Engineering, University of Toronto, Ont., Canada.

M. Trefler is with the Department of Radiology, Division of Radiological Sciences, School of Medicine, University of Miami, Miami, FL 33101.

[1] An approximation was made to make the system linear: since the values of the linear attenuation coefficients, or at least their variations from point to point, are small, the exponential representing the attenuation of X-rays through matter can be approximated by the linear terms of its Taylor series expansion [1], [2].

0278-0062/85/0300-0001$01.00

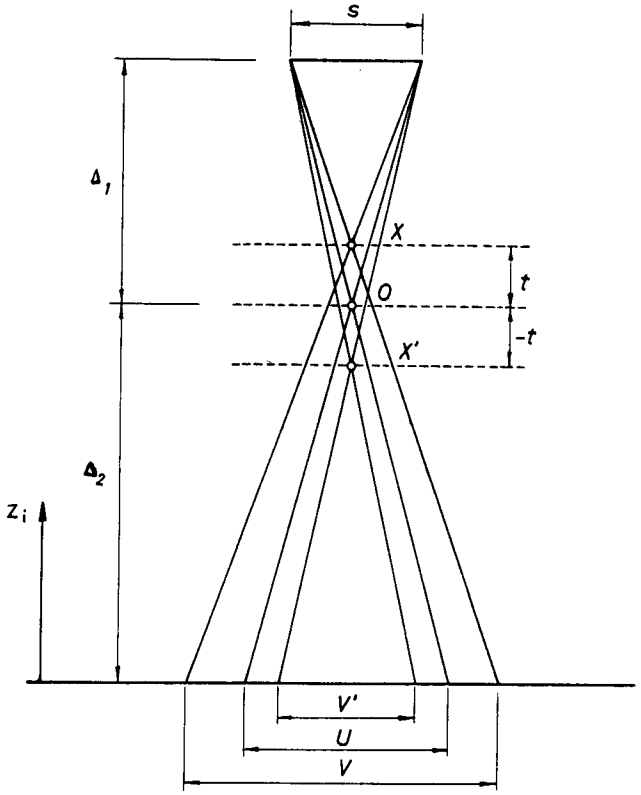

Fig. 1. Blur formation in the radiologic process.

image, I_B is a constant, $H_i(f_x, f_y, z_i)$ is the overall transfer function of the ith layer at a depth z_i, and $F_\mu(f_x, f_y, z_i)$ is the Fourier transform of the (scaled) distribution of linear absorption coefficients in the ith layer (cf. [1]).

Equation (1) applies to standard tomography, conventional radiology, or tomographic filtering by using the transfer function given in (2), (3), or (4), respectively (cf. [1]).

Standard Tomography:

$$H_i^{ST}(f_x, f_y, z_i) = \left[\frac{z_i - d}{z_i - \Delta_2}\,\frac{\Delta_1}{d}\right]^2 \cdot \iint I_0\left\{\frac{z_i - d}{z_i - \Delta_2}\,\frac{\Delta_1}{d}\,x, \frac{z_i - d}{z_i - \Delta_2}\,\frac{\Delta_1}{d}\,y\right\} \cdot e^{-j2\pi(f_x x + f_y y)}\,dx\,dy \tag{2}$$

Conventional Radiology:

$$H_i^{CR}(f_x, f_y, z_i) = \left[\frac{z_i - d}{z_i}\right]^2 \iint I_0\left\{\frac{z_i - d}{z_i}\,x, \frac{z_i - d}{z_i}\,y\right\} \cdot e^{-j2\pi(f_x x + f_y y)}\,dx\,dy \tag{3}$$

Tomographic Filtering:

$$H_i^{TF}(f_x, f_y, z_i) = \frac{\left[\frac{z_i - d}{z_i}\right]^2 \iint I_0\left\{\frac{z_i - d}{z_i}\,x, \frac{z_i - d}{z_i}\,y\right\} e^{-j2\pi(f_x x + f_y y)}\,dx\,dy}{\left[\frac{z_t - d}{z_t}\right]^2 \iint I_0\left\{\frac{z_t - d}{z_t}\,x, \frac{z_t - d}{z_t}\,y\right\} e^{-j2\pi(f_x x + f_y y)}\,dx\,dy} \tag{4}$$

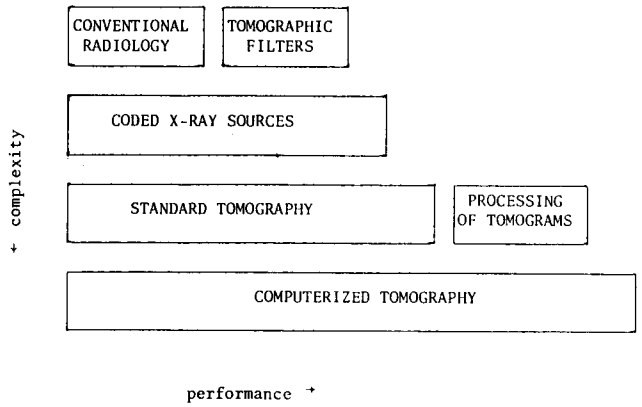

Fig. 2. Relative standing of several radiologic procedures (subjective, not to scale).

where the depth of the tomograhic layer is $z_t = \Delta_2$, $d \triangleq \Delta_1 + \Delta_2$, and $I_0(\cdot, \cdot)$ is the exposure function, that is, either the intensity distribution of the movement of an X-ray source in standard tomography or the focal spot X-ray distribution in conventional tomography and tomographic filtering [1]-[3].

In spite of the fact that the equations of image formation in standard tomography, conventional radiology, and tomographic filtering are similar, there are fundamental physical differences among these methods. A good objective indication of performance of a radiologic system is given by the overall transfer functions of the layers in the object. The qualitative differences among these transfer functions are discussed in [1] while various quantitative performance parameters are examined in this paper (a summary also appears in [1], [3]).

As shown in [1], of particular interest are the characteristics of the transfer function in (4) for tomographic filtering when the depth z_i varies. Indeed, for layers between the focal spot and the plane of cut this transfer function has low-pass characteristics, while between the plane of cut and the film has high-pass characteristics [1].

The implementation of (4) is discussed in detail in [2] and [12], where techniques are proposed to prevent noise amplification due to zeros or low values in the denominator in (4).

III. Comparative Assessment of Tomographic Filtering

In this section a comparative assessment of tomographic filtering is produced taking as benchmarks two well established radiologic procedures: standard tomography and conventional radiology. Tomographic filtering is an extension of conventional radiology which can improve its quality enhancing depth information, thus approaching the quality of standard tomography. This is shown diagrammatically in Fig. 2. The relative standing and the tradeoffs among these three methods are described in this section in more detail.

For completeness, Fig. 2 shows other methods that can be used to recover three-dimensional information, but which are not discussed in this paper. Coded X-ray sources (e.g., a Fresnel zone plate pattern) produce a shadow image of the object, but in a coded form. Decoding is done using optical techniques and only a thin slice of the object is in focus at one time, but other slices may be brought into focus by changing lens positions in the reconstruction system. Alternatively, digital techniques can also be used in the reconstruction. The same idea of tomographic filters for conventional radiology could be applied to standard tomograms, thus changing the plane of cut [1]. Finally, computerized tomography techniques use more than one X-ray image or projection of the object to reconstruct any layer by digital or optical methods.

The comparison between standard tomography, conventional radiology, and tomographic filtering is made on the basis of the following evaluation criteria: the exposure angle, the thickness of the cut, the rate of change of the transfer function, the signal-to-noise ratio, and the radiation dose. Although the ultimate measure of performance is the diagnosis by a radiologist, the comparisons will be kept as objective as possible without going into details of clinical value and operational procedures which tend to be subjective.

A. The Exposure Angle

The most evident quantitative difference between a tomographic filtration process and standard tomography is the size of the focal spot in radiology as opposed to the extension of the movement of the X-ray source in standard tomography. They have a direct effect on the extension of the blur and therefore on the thickness of the tomographic layer. A typical size for a focal spot is of the order of 1 or 2 mm while the movement of an X-ray source varies from a few mm in zonography[2] up to 500 mm and more in standard tomography.

In tomography it is more usual to give the exposure angle rather than the extension of the movement of the X-ray source. The exposure angle is defined as the angle through which the projecting ray of a central point of the plane of cut moves during the exposure.

In conventional radiology and, therefore, in a tomographic filtration process, the exposure angle depends on the size of the focal spot. With a typical focal spot size of 2 mm and focal spot to plane of cut distance of 1000 mm, the exposure angle is 2 arctan 0.001 = 0.002 radians. The following list gives the range of exposure angles for various tomographic procedures.

Tomographic filtration process	5′-15′
Zonography	1°-5°
Standard tomography	10°-60°
Transversal tomography	120°-170°

Thus, in terms of the exposure angle, a tomographic filtration process is closer to zonography than to any other tomographic technique.

B. The Thickness of the Cut

Conventionally, in tomography the thickness of the cut is defined as the distance between the two levels which have a tomographic blurring $B \geqslant B_m$ that is insufficiently large to be noticeable in the presence of the usual radiographic blurrings B_m [4, p. 355]. In standard tomography a reasonable choice for B_m is 0.7 mm [4, p. 355]. This is a subjective definition[3] and it depends on the amount of other blurrings such as those due to the focal-spot intensity distribution and patient movement. In a tomographic filtration process the tomographic blur is based on the focal-spot intensity distribution, and the blur due to patient movement is negligible because the exposure time is short. Therefore, the threshold B_m in a tomographic filtration process should be chosen to be less than 0.7 mm. Since the definition of "thickness of cut" is already so fuzzy, here we neglect the effects of the focal-spot intensity distribution and the high-pass filter characteristics on layers on the film side. Hence, from Fig. 1 an indication of the differential blur that will remain after processing can be expressed as

$$|V - U| = \left| s\,\frac{\Delta_2 + t}{\Delta_1 - t} - s\,\frac{\Delta_2}{\Delta_1} \right| = s\left|\frac{(\Delta_1 + \Delta_2)\,t}{(\Delta_1 - t)\,\Delta_1}\right|$$

where s is the size of the focal spot and t is the distance from a layer to the tomographic layer.

Therefore, the thickness of the tomographic layer is given by

$$2t = \frac{2B_m \Delta_1^2}{s(\Delta_1 + \Delta_2) + B_m \Delta_1}$$

or in terms of the exposure angle Θ_m

$$2t = \frac{2B_m \Delta_1}{\Theta_m(\Delta_1 + \Delta_2) + B_m}\,. \tag{5}$$

We see that the tomographic blur $|V - U|$ is proportional to the size of the focal spot. Since a typical size for the focal spot is of the order of 2 mm, while the movement of an X-ray source in standard tomography is of the order of 500 mm, we infer that the results of a TFP cannot be as good as those of standard tomography. Nevertheless, the purpose of a TFP is to improve a radiograph with respect to three-dimensional information and not to produce a complete and accurate three-dimensional reconstruction for which better techniques exist.

In standard tomography the thickness of the cut is of the order of a few millimeters, in zonography it is of the order of a few centimeters, and in a tomographic filtration process even larger. However, for a fair comparison the value of B_m should be changed accordingly, as previously discussed. Indeed, the minimum discernible blur in standard tomography has a fixed component due to focal spot size and patient movements, which are practically nonexistent in tomographic filtering.

[2] Zonography is essentially standard tomography using smaller movements of the X-ray source [4, p. 360], [5, ch. 14], [6], [7]. Other narrow-angle tomographic techniques are the following [5, pp. 7-8 and pp. 300-311]: stereozonography, narrow-angle stratigraphy, and orthotomography.

[3] A more objective definition has been proposed in [8] in terms of the amount of attenuation desired and the spatial frequencies of interest.

Therefore, let the minimum discernible blur in tomographic filtered radiographs be B_m/K_f where B_m is 0.7 mm as usual in standard tomography and K_f is an appropriate constant greater than one. Because of the lack of experimental evidence we can only make an educated guess about the value of K_f; we assume that a realistic value is at least $K_f = 2$. Furthermore, computer processed radiographs can be readily manipulated, magnified, contrast enhanced, etc. In particular, magnification is important here because it is inversely proportional to the minimum discernible blur, namely $B_m/K_f/K_m$, where K_m is the magnification of the processed radiograph (not the radiologic magnification but the display magnification).[4] Since only a small portion of the radiograph, say 1 to 4 in^2, will be processed at a time by the tomographic filter, this area can be displayed at full resolution and thus magnification can be as high as 20; nevertheless, in this calculation we will assume a lower value, say $K_m = 10$.

Consequently, taking into account the constants K_m and K_f, (5) becomes (6) for tomographic filtering

$$2t = \frac{2B_m \Delta_1}{K_f K_m \theta_m (\Delta_1 + \Delta_2) + B_m} . \tag{6}$$

Hence, assuming $B_m = 0.7$ mm, $\Delta_1 = \Delta_2 = 1000$ mm, $K_f = 2$, $K_m = 10$, and $\theta_m = 10'$, the thickness of the cut is $2t = 12$ mm for the tomographic filtration process. On the other hand in zonography, with $K_f = K_m = 1$ and $\theta_m = 3°$ we obtain $2t = 13$ mm and in standard tomography with $\theta_m = 35°$ we obtain $2t = 1$ mm. Of course, the display magnification of standard tomograms and zonograms would also further reduce the apparent thickness of the cut, however, this technique would not work as well in these cases because there are other blurrings present (due to focal spot and patient movement).

It may seem that the thinner the cut the better. Nevertheless, there are cases where a thick cut is preferred. Each special tomographic technique has its own predilective applications [5, ch. 14]. Interactive tomographic filtering offers the advantage that by computer manipulation the apparent thickness of the cut can be changed by magnification at the expense of reducing the field of view.

C. The Rate of Change of the Transfer Function

To further quantify the difference between tomographic filtering and standard tomography we propose a new measure based on the contrast between layers. Indeed, we will calculate and compare the rates of change of the magnitude/modulation transfer functions in (2) and (4) from layer to layer for a specific type of exposure function $I_0(\cdot, \cdot)$.

Equations (2)-(4) can be simplified by introducing $F_{I_0}(f_x, f_y)$, the two-dimensional Fourier transform of $I_0(x, y)$, and using the scaling property; thus we obtain (7)-(9), respectively.

$$H_i(f_x, f_y, z_i) = F_{I_0}\left(\frac{z_i - \Delta_2}{z_i - d}\frac{d}{\Delta_1} f_x, \frac{z_i - \Delta_2}{z_i - d}\frac{d}{\Delta_1} f_4\right) \tag{7}$$

$$H_i(f_x, f_y, z_i) = F_{I_0}\left(\frac{z_i}{z_i - d} f_x, \frac{z_i}{z_i - d} f_y\right) \tag{8}$$

$$H_i(f_x, f_y, z_i) = \frac{F_{I_0}\left(\frac{z_i}{z_i - d} f_x, \frac{z_i}{z_i - d} f_y\right)}{F_{I_0}\left(\frac{z_t}{z_t - d} f_x, \frac{z_t}{z_t - d} f_y\right)} \tag{9}$$

where (9) is valid in a finite region around the origin in the frequency plane.

We have now reached the point where to proceed with the comparison we must make some assumption about the function $I_0(x, y)$, or equivalently, its Fourier transform. It has been discussed that a Gaussian function is a good approximation to the intensity distribution in actual focal spots [1]. In standard tomography $I_0(x, y)$ is not Gaussian in general because it represents the movement of the X-ray source whose intensity is usually constant during the exposure. Nevertheless, to make the evaluation tractable mathematically, for the purpose of this comparison we will assume identical functions $I_0(x, y)$ leading to (7), (8), and (9), because what we want to compare is the rate of change of the transfer function with respect to the mode of operation (i.e., movement or filtering) rather than with respect to the actual $I_0(x, y)$. Thus, in the specific case the $I_0(x, y)$ is a circularly-symmetric Gaussian function [see (10)], $F_{I_0}(f_x, f_y)$ is also a Gaussian function [see (11)].

$$I_0(x, y) = \exp\{-\sigma^2 x^2 - \sigma^2 y^2\} \tag{10}$$

$$F_{I_0}(f_x, f_y) = \frac{\pi}{\sigma^2} \exp\left\{-\left(\frac{f_x}{\sigma/\pi}\right)^2 - \left(\frac{f_y}{\sigma/\pi}\right)^2\right\} . \tag{11}$$

Substituting (11) into (7), (8), and (9), we obtain (12), (13), and (14), respectively.

$$H_i(f_x, f_y, z_i) = \frac{\pi}{\sigma^2} \exp\left\{-\left[\frac{\pi}{\sigma}\frac{z_i - \Delta_2}{z_i - d}\frac{d}{\Delta_1}\right]^2 (f_x^2 + f_y^2)\right\} \tag{12}$$

$$H_i(f_x, f_y, z_i) = \frac{\pi}{\sigma^2} \exp\left\{-\left[\frac{\pi}{\sigma}\frac{z_i}{z_i - d}\right]^2 (f_x^2 + f_y^2)\right\} \tag{13}$$

$$H_i(f_x, f_y, z_i) = \exp\left\{-\left(\frac{\pi}{\sigma}\right)^2 \left[\left(\frac{z_i}{z_i - d}\right)^2 - \left(\frac{z_t}{z_t - d}\right)^2\right] \cdot (f_x^2 + f_y^2)\right\} \tag{14}$$

These formulas clearly show the low pass nature of the transfer functions of standard tomography (12) and conventional radiology (13). On the other hand the overall transfer function of a tomographic filtration process (14) can be low pass (if $z_i > z_t$) or high pass (if $z_i < z_t$) depending on the layer concerned. This is discussed in more detail in [1].

The rate of change of the transfer function with respect to

[4] Display magnification on a CRT screen is similar to the common practice used reading radiographs where the radiologist can change the film to eye distance in order to improve edge visibility at the expense of increasing the visibility of the noise. If the digitized image has enough resolution, display magnification can bring out details which otherwise would not be seen.

z_i is given by the first derivative of $H_i(f_x, f_y, z_i)$ with respect to z_i. However, since the transfer functions in (12) and (14) are both exponential functions, we will use as a measure of the rate of change of the transfer function from layer to layer the derivative of the coefficient of $(f_x^2 + f_y^2)$ with respect to z_i. The derivative of the coefficient in (12) is given in (15) and the derivative of the coefficient in (14) is given in (16).

$$y_{ST}(z_i) = 2\left(\frac{\pi}{\sigma}\right)^2 \frac{d^2}{\Delta_1} \frac{z_i - \Delta_2}{(d - z_i)^3} \tag{15}$$

$$y_{TF}(z_i) = 2\left(\frac{\pi}{\sigma}\right)^2 d \frac{z_i}{(d - z_i)^3} \tag{16}$$

Therefore, in standard tomography the slope $y_{ST}(z_i)$ is negative if $z_i < \Delta_2$ (i.e., between the film and the tomographic layer) and positive if $z_i > \Delta_2$ (i.e., between the tomographic layer and the focal spot). This change of sign of the slope is due to the fact that the coefficient itself stays positive when the tomographic layer is crossed and it is zero at the tomographic layer (i.e., the function has a minimum). On the other hand, in tomographic filtering the slope $y_{TF}(z_i)$ is always positive because it is the coefficient that changes sign when crossing the tomographic layer. The ratio of the two slopes is given in (17).

$$\Gamma(z_i) = \frac{y_{TF}(z_i)}{y_{ST}(z_i)} = \frac{\Delta_1}{d} \frac{z_i}{z_i - \Delta_2} \tag{17}$$

Hence, whenever $|\Gamma(z_i)| > 1$ the rate of change of the transfer function from layer to layer is greater in a tomographic filtration process than in the equivalent system using standard tomography, and vice versa when $|\Gamma(z_i)| < 1$. The ranges of z_i in each case are easily calculated

$$0 < z_i < \frac{d\Delta_2}{2d - \Delta_2} \qquad |\Gamma(z_i)| < 1 \tag{18}$$

$$\frac{d\Delta_2}{2d - \Delta_2} < z_i < d \qquad |\Gamma(z_i)| > 1. \tag{19}$$

Consequently, for the layers between the focal spot and the layer at a distance $d\Delta_2/(2d - \Delta_2)$ from the film, the transfer function in a tomographic filtration process varies faster from layer to layer than in the equivalent system using standard tomography. It can be shown that the interval $d\Delta_2/(2d - \Delta_2) < z_i < d$ always contains the tomographic layer $z_i = \Delta_2$, hence, in a region around the tomographic layer, tomographic filtering gives better contrast between layers than standard tomography.

Examples (all distances in mm)

d	Δ_2	$d\Delta_2/(2d - \Delta_2) < z_i < d$		$\frac{200\,\Delta_1}{d + \Delta_1}$ (percent)
1000	500	333.3	$< z_i < 1000$	66
1000	400	250	$< z_i < 1000$	75
1000	600	428.6	$< z_i < 1000$	57

where the last column represents the percentage of the space between the focal spot and the film where tomographic filtering gives better contrast.

Specific values of the slopes can be obtained by substituting values in (15) and (16). Indeed, assuming $\sigma = 2$, $d = 1000$, and $\Delta_1 = \Delta_2 = 500$, we obtain the following results:

z_i	$y_{ST}(z_i)$ (percent)	$y_{TF}(z_i)$ (percent)
0	-0.49	0
100	-0.54	0.07
200	-0.58	0.15
300	-0.57	0.43
400	-0.46	0.91
500	0	1.97
600	1.5	4.6
700	7.3	12.8
800	37	49
900	395	444
1000	∞	∞

The previous analysis has assumed identical exposure functions $I_0(x, y)$ in each case as defined in (10). We are now going to repeat the analysis assuming different σ's in (10) both for tomographic filtering and standard tomography, but the shape of $I_0(x, y)$ is still the same in both cases, a Gaussian function. Equations (15) and (16) thus become (20) and (21), respectively.

$$y_{ST}(z_i) = 2\left(\frac{\pi}{\sigma_{ST}}\right)^2 \frac{d^2}{\Delta_1} \frac{z_i - \Delta_2}{(d - z_i)^3} \tag{20}$$

$$y_{TF}(z_i) = 2\left(\frac{\pi}{\sigma_{TF}}\right)^2 d \frac{z_i}{(d - z_i)^3}. \tag{21}$$

Their ratio is

$$\Gamma(z_i) = \frac{y_{TF}(z_i)}{y_{ST}(z_i)} = \left(\frac{\sigma_{ST}}{\sigma_{TF}}\right)^2 \frac{\Delta_1}{d} \frac{z_i}{z_i - \Delta_2} \tag{22}$$

and $|\Gamma(z_i)| > 1$, whenever the following inequality is satisfied:

$$\frac{\sigma_{TF}^2 d\Delta_2}{\sigma_{TF}^2 d + \sigma_{ST}^2 \Delta_1} < z_i < \frac{\sigma_{TF}^2 d\Delta_2}{\sigma_{TF}^2 d - \sigma_{ST}^2 \Delta_1}. \tag{23}$$

Assuming $\sigma_{TF} = 2$ and $\sigma_{ST} = 0.005$, $d = 1000$ and $\Delta_1 = \Delta_2 = 500$, we obtain

$$499.9 < z_i < 500.1.$$

Thus, now the region where the rate of change of the transfer function of a tomographic filtration process is greater than that of standard tomography is very narrow indeed, practically negligible; however, it always includes the plane of cut. This suggests that the use of the term "thickness of the cut" may not be as relevant in tomographic filtering as it is in standard tomography.

The absolute values of the slopes $y_{ST}(z_i)$ and $y_{TF}(z_i)$ in the examples given previously now differ by an additional factor

$$\left(\frac{\sigma_{TF}}{\sigma_{ST}}\right)^2 = \left(\frac{2}{0.005}\right)^2 = 160\,000$$

in favor of standard tomography because of the different size (scalings) used in this example.

Hence, the percentage of the space between focal spot and film in favor of tomographic filtering is now

$$\frac{200\sigma_{TF}^2\sigma_{ST}^2\Delta_1\Delta_2}{\sigma_{TF}^4 d^2 - \sigma_{ST}^4\Delta_1^2} \text{ percent.} \tag{24}$$

If $\sigma_{TF} \gg \sigma_{ST}$ (24) can be approximated by (25).

$$\frac{200\sigma_{ST}^2\Delta_1\Delta_2}{\sigma_{TF}^2 d^2} \text{ percent} \tag{25}$$

which in the previous example amounts only to 0.003 percent.

In conclusion then, the operation of tomographic filtering gives better layer contrast than standard tomography in an interval around the plane of cut. However, if the normal sizes of the exposure function are taken into consideration, the performance of standard tomography is by far better because that interval is negligible. Furthermore, this analysis does not include any artifacts that may appear due to out-of-focus layers.

D. The Signal to Noise Ratio

In this section, tomographic filtering is evaluated further by studying the effects that system parameters such as focal spot size have on the results; thus allowing comparisons between systems. This evaluation is done in terms of the signal-to-noise ratio, which is defined as the ratio of the power of the signal from the plane of cut, if it was the only one present in the object, and the power of the noise contributed by all other planes. The signal to noise ratio,[5] as defined here, provides another measure of the contrast of the image of the plane of cut with respect to the others.

In this analysis the object, represented by the distribution of linear attenuation coefficients $\mu(x_i, y_i, z_i)$, is considered to be a random process with parameter space x_i, y_i, z_i. It is convenient to express $\mu(x_i, y_i, z_i)$ as a function of the coordinates on the film plane, that is (cf. [1])

$$x_i = \frac{d - z_i}{d} x \quad \text{and} \quad y_i = \frac{d - z_i}{d} y.$$

Therefore

$$\mu(x_i, y_i, z_i) = \mu\left(\frac{d - z_i}{d} x, \frac{d - z_i}{d} y, z_i\right).$$

Let the two-dimensional correlation function of this random process with respect to the first two parameters be

$$R_\mu\left(\frac{d - z_i}{d} x, \frac{d - z_i}{d} y, z_i\right). \tag{26}$$

The two-dimensional power spectral density function of this random process is given by the two-dimensional Fourier transform of (26), which is given in (27).

$$S_{\mu_i}(f_x, f_y, z_i) = \iint R_\mu\left(\frac{d - z_i}{d} x, \frac{d - z_i}{d} y, z_i\right) \cdot e^{-j2\pi(f_x x + f_y y)}\, dx\, dy = \left(\frac{d}{d - z_i}\right)^2 S_\mu\left(\frac{d}{d - z_i} f_x, \frac{d}{d - z_i} f_y, z_i\right) \tag{27}$$

where S_μ is the two-dimensional Fourier transform of R_μ. For example, if the random process is white noise S_{μ_i} is given by (28).

$$S_{\mu_i}(f_x, f_y, z_i) = \left(\frac{d}{d - z_i}\right)^2 S_o \tag{28}$$

where S_o is a constant for all f_x, f_y, and z_i. If this noise is band limited between $-W$ and W, the power spectral density function is

$$S_{\mu_i}(f_x, f_y, z_i) = \begin{cases} \left(\frac{d}{d - z_i}\right)^2 S_o & \text{for } -W_i \leqslant f_x,\ f_y \leqslant W_i \\ 0 & \text{otherwise} \end{cases} \tag{29}$$

where

$$W_i = \frac{d - z_i}{d} W.$$

Following a derivation similar to that in [1], it can be shown that imaging the random process $\mu(x_i, y_i, z_i)$ results in an image which is also a random process with power spectral density $S_g(f_x, f_y)$ given by (30).

$$S_g(f_x, f_y) = I_B^2 \delta(f_x, f_y) - \int_0^d |H_i(f_x, f_y, z_i)|^2\, S_{\mu_i}(f_x, f_y, z_i)\, dz_i \tag{30}$$

where I_B is a constant and $H_i(f_x, f_y, z_i)$ is the overall two-dimensional transfer function of the ith layer at a depth z_i. I_B is given by the integral of the exposure function $I_o(x_o, y_o)$ (cf. [1]) divided by the dc gain of the tomographic filter, if present; H_i is given by (2), (3), or (4), depending on the type of radiologic process considered; and S_{μ_i} is given by (29). We can now determine the power in the image which is given by (31).

$$P = \iint S_g(f_x, f_y)\, df_x\, df_y. \tag{31}$$

To determine the signal-to-noise ratio we separate the power component due to the image of the tomographic layer (P_t) and the noise power due to the other layers (P_n). It is also useful to separate the noise power due to layers between the anode and the plane of cut (P_a) and the noise power due to

[5]The use of the signal-to-noise ratio as a measure of performance for digital tomographic filters was suggested by Dr. M. L. G. Joy, Institute of Biomedical Engineering, University of Toronto, Canada.

layers between the plane of cut and the film (P_f). These powers are related as follows:

$$P = P_t + P_n = P_t + P_a + P_f. \tag{32}$$

If z_t is the depth of the plane of cut and $2t$ is its thickness, expressions for these powers can be obtained from (30), as indicated in (33)–(36).

$$P = p(z_f, z_a) \tag{33}$$

$$P_t = p(z_t - t, z_t + t) \tag{34}$$

$$P_a = p(z_t + t, z_a) \tag{35}$$

$$P_f = p(z_f, z_t - t) \tag{36}$$

where the function $p(z_1, z_2)$ is defined in (37) and the depths z_a and z_f determine the limits of the object ($0 \leqslant z_f \leqslant z_a \leqslant d$).

$$p(z_1, z_2) = \int_{z_1}^{z_2} \left[\iint |H_i(f_x, f_y, z_i)|^2 \cdot S_{\mu_i}(f_x, f_y, z_i)\, df_x\, df_y \right] dz_i. \tag{37}$$

The corresponding signal-to-noise ratios (SNR) can then be calculated as follows:

$$\text{SNR} = \frac{P_t}{P_n} = \frac{P_t}{P_a + P_f} = \frac{p(z_t - t, z_t + t)}{p(z_t + t, z_a) + p(z_f, z_t - t)} \tag{38}$$

$$\text{SNR}_a = \frac{P_t}{P_a} = \frac{P(z_t - t, z_t + t)}{p(z_t + t, z_a)} \tag{39}$$

$$\text{SNR}_f = \frac{P_t}{P_f} = \frac{p(z_t - t, z_t + t)}{p(z_f, z_t - t)}. \tag{40}$$

It is easy to show that

$$\frac{1}{\text{SNR}} = \frac{1}{\text{SNR}_a} + \frac{1}{\text{SNR}_f} \tag{41}$$

or

$$\text{SNR} = \frac{\text{SNR}_a \times \text{SNR}_f}{\text{SNR}_a + \text{SNR}_f}. \tag{42}$$

To proceed with the evaluation, we consider the case where the intensity distribution in the focal spot is a Gaussian function, as justified previously [recall (10)], and the object is band-limited white noise [recall (29)] with S_o small, to conform with the approximations made in the derivation of (1). Therefore

$$\iint I_0(x_0, y_0)\, dx_0\, dy_0 = \iint \exp\{-\sigma^2 x_0^2 - \sigma^2 y_0^2\}\, dx_0\, dy_0 = \frac{\pi}{\sigma^2}. \tag{43}$$

Although the SNR does not depend on the energy in the focal spot, we consider the case where this energy is a constant independent of σ, to allow a more meaningful comparison of powers when σ varies. Consequently,

$$I_0(x_0, y_0) \triangleq \frac{\sigma^2}{\pi} \exp\{-\sigma^2 x_0^2 - \sigma^2 y_0^2\}$$

and

$$\iint I_0(x_0, y_0)\, dx_0\, dy_0 = 1.$$

And if the DC gain of the tomographic filter is also normalized to unity, then $I_B = 1$ in all cases. Hence,

$$H_i(f_x, f_y, z_i) = \exp\left\{ -\left(\frac{\pi}{\sigma}\right)^2 B_i(f_x^2 + f_y^2) \right\} \tag{44}$$

where (44) is derived from (12), (13), and (14), and B_i is given by the following list:

Procedure	B_i	
Standard tomography	$\left(\frac{z_i - \Delta_2}{z_i - d}\,\frac{d}{\Delta_1}\right)^2$	(45)
Conventional radiology	$\left(\frac{z_i}{z_i - d}\right)^2$	(46)
Tomographic filtering	$\left(\frac{z_i}{z_i - d}\right)^2 - \left(\frac{z_t}{z_t - d}\right)^2$	(47)

and finally

$$S_{\mu_i}(f_x, f_y, z_i) = \left(\frac{d}{d - z_i}\right)^2 S_o \quad \text{for } -W_i \leqslant f_x,\ f_y \leqslant W_i \tag{48}$$

where

$$W_i = \frac{d - z_i}{d} W.$$

Also, to make the results more general, let us assume that the tomographic filter is band limited between $-f_c$ and f_c, by a low-pass filter whose function is to reduce noise.

Now we can calculate the following integral [refer to (37)].

$$p(z_1, z_2) = \int_{z_1}^{z_2} \left[\iint |H_i(f_x, f_y, z_i)|^2 \cdot S_{\mu_i}(f_x, f_y, z_i)\, df_x\, df_y \right] dz_i. \tag{49}$$

Substituting (44) and (48) into (49), we obtain

$$p(z_1, z_2) = \int_{z_1}^{z_2} \left[\int_{-f_m}^{f_m} \int_{-f_m}^{f_m} \cdot \exp\left\{ -2\left(\frac{\pi}{\sigma}\right)^2 B_i(f_x^2 + f_y^2) \right\} \cdot \left(\frac{d}{d - z_i}\right)^2 S_o\, df_x\, df_y \right] dz_i \tag{50}$$

$$= \frac{S_o}{2}\left(\frac{d\sigma}{\pi}\right)^2 \int_{z_1}^{z_2} \frac{1}{(d-z_i)^2}\,\frac{1}{|B_i|} \cdot \Phi^2\left\{2\left(\frac{\pi}{\sigma}\right)^2 B_i f_m^2\right\} dz_i \qquad (51)$$

where $f_m = \min(f_c, W_i)$ and $\Phi(x)$ is a generalized form of the error function to include positive exponentials, as defined in (52).

$$\Phi(x) \triangleq \frac{2}{\sqrt{\pi}} \int_0^{\sqrt{|x|}} e^{-\mathrm{sgn}(x)\,u^2}\, du \qquad (52)$$

$$= \frac{2}{\sqrt{\pi}}\left[\sum_{n=0}^{\infty} \frac{(-\mathrm{sgn}(x))^n\,|x|^{(2n+1)/2}}{n!\,(2n+1)}\right]. \qquad (53)$$

When $x > 0$, the function $\Phi(x)$ is the well known error function for the square root of the argument, that is

$$\Phi(x) = \mathrm{erf}(\sqrt{x}) \quad \text{for } x > 0. \qquad (54)$$

When $x < 0$, the function $\Phi(x)$ is calculated here using the power series in (53) which is absolutely convergent for all real values of x.

Therefore, (51) can be calculated to determine the signal-to-noise ratios in (38)-(40). Since the SNR is a function of several parameters characteristic of the radiologic process such as S_o, σ, d, z_t, W, and f_c, whose influence over the SNR is not obvious, (38)-(40) were evaluated for more than 4000 cases using (51). The integral in (51) was calculated using Simpson's rule with 1 mm intervals. The value of d was 1000 mm in all cases. The size of the focal spot, determined by σ (the larger σ is, the smaller the focal spot is), was varied between $\sigma = 2$ and $\sigma = 10$ (in mm^{-1}) for all combinations of the other parameters. The total thickness of the object was 264 mm in all cases (assumed to be the thickness of a typical chest). The plane of cut was always in the center of the object but the position of the object was varied to observe the effect its position would have on the SNR. Thus, three cases were considered: $z_t = 500$ mm (object is exactly in the middle between the focal spot and the film), $z_t = 520$ mm (object is closer to the focal spot), and $z_t = 480$ mm (object is closer to the film). The thickness of the tomographic layer ($2t$) was varied between 4 mm and 240 mm ($t = 2, 10, 20, 50, 100$, and 120 mm).

Two types of object power spectra were considered: white noise ($W = \infty$) and band-limited white noise (two different bandwidths: $W = 4$ and 5 cycles/mm), with $S_o = 10^{-2}$, 10^{-5}, and 10^{-8} [recall (48)]. The image given by each type of object was band limited by a low-pass filter using two cutoff frequencies $f_c = 3$ and 4 cycles/mm. The correspondence between object bandwidth and filter bandwidth was as follows (all units in cycles/mm):

W	f_c
∞	3
∞	4
4	3
5	4

TABLE I
THE SIGNAL-TO-NOISE RATIOS VERSUS THE THICKNESS OF THE CUT

Fixed parameters: d = 1000 mm, z_t = 500 mm, σ = 10, W = 5 cycles/mm, f_c = 4 cycles/mm.

t(mm) =	2	10	20	50	100	120
Standard tomography						
SNR	0.017	0.089	0.19	0.67	3.6	11.
SNR_a	0.033	0.18	0.39	1.3	7.1	23.
SNR_f	0.033	0.18	0.39	1.3	7.1	23.
Conventional radiology						
SNR	0.015	0.081	0.18	0.60	3.1	9.8
SNR_a	0.036	0.19	0.43	1.5	8.3	27.
SNR_f	0.026	0.14	0.3	0.99	4.9	15.
Tomographic filtering						
SNR	0.013	0.068	0.15	0.48	2.3	7.4
SNR_a	0.045	0.24	0.55	2.1	13.	47.
SNR_f	0.018	0.093	0.2	0.62	2.8	8.7

These frequencies were chosen so that when the object is band-limited white noise, the low-pass filter has no effect, that is, the image is only band limited by the bandwidth of the object itself.

Since it is impractical to include here all the results obtained, only sufficient summary tables are produced to support the conclusions.

The following data were selected from the results to show the effect on the SNR by parameters such as the nominal thickness of the cut, the position of the object between focal spot and film, the size of the focal spot, and the bandwidths of the object and the low-pass filter. These selected results are given in Tables I-V.

Table I shows the variation of the SNR with the thickness of what is considered to be the tomographic layer. It is clear that the SNR (also SNR_a and SNR_f) increases with the thickness of the tomographic layer, as expected, because of the definition of the SNR [recall (38), (39) and (40)].

Table II shows the variations of the SNR with respect to the position of the object between the focal spot and the film. When the object moves closer to the focal spot the SNR increases in standard tomography but in conventional radiology and tomographic filtering the SNR decreases. To explain this effect we look more closely at the variations of SNR_a and SNR_f. In conventional radiology and tomographic filtering, SNR_a increases and SNR_f decreases when the object is moved towards the focal spot. Since SNR_f dominates over SNR_a ($SNR_f < SNR_a$) SNR also decreases.

A similar argument is in order with regard to the size of the focal spot, as shown in Table III. Indeed, increasing the size of

TABLE II
THE SIGNAL-TO-NOISE RATIOS VERSUS THE POSITION OF THE OBJECT

Fixed parameters: d = 1000 mm, σ = 10, t = 20 mm, W = 5 cycles/mm, f_c = 4 cycles/mm

z_t (mm) =	480	500	520
Standard tomography			
SNR	0.193	0.194	0.195
SNR_a	0.386	0.388	0.391
SNR_f	0.386	0.388	0.391
Conventional radiology			
SNR	0.177	0.176	0.176
SNR_a	0.426	0.427	0.428
SNR_f	0.301	0.300	0.299
Tomographic filtering			
SNR	0.150	0.145	0.140
SNR_a	0.536	0.551	0.567
SNR_f	0.209	0.197	0.185

TABLE III
THE SIGNAL-TO-NOISE RATIOS VERSUS THE SIZE OF THE FOCAL SPOT

Fixed parameters: d = 1000 mm, z_t = 500 mm, t = 20 mm, W = 5 cycles/mm

σ =	2	4	6	8	10
Standard tomography					
SNR	0.490	0.270	0.221	0.203	0.194
SNR_a	0.980	0.541	0.442	0.406	0.388
SNR_f	0.980	0.541	0.442	0.406	0.388
Conventional radiology					
SNR	0.164	0.165	0.168	0.173	0.176
SNR_a	0.470	0.470	0.465	0.447	0.427
SNR_f	0.253	0.254	0.264	0.283	0.300
Tomographic filtering					
SNR	$7.7\ 10^{-23}$	$9.5\ 10^{-5}$	$3.5\ 10^{-2}$	0.11	0.15
SNR_a	$1.3\ 10^{+2}$	2.1	0.96	0.67	0.55
SNR_f	$7.7\ 10^{-23}$	$9.5\ 10^{-5}$	$3.5\ 10^{-2}$	0.13	0.20

TABLE IV
THE SIGNAL-TO-NOISE RATIOS VERSUS THE BANDWIDTH OF THE OBJECT

Fixed parameters: d = 1000 mm, z_t = 500 mm, σ = 10, t = 20 mm.

W(cycles/mm) =	4	5
Standard tomography		
SNR	0.189	0.194
SNR_a	0.377	0.388
SNR_f	0.377	0.388
Conventional radiology		
SNR	0.178	0.176
SNR_a	0.408	0.430
SNR_f	0.316	0.300
Tomographic filtering		
SNR	0.164	0.145
SNR_a	0.478	0.550
SNR_f	0.250	0.200

TABLE V
THE SIGNAL-TO-NOISE RATIOS VERSUS THE CUTOFF FREQUENCY

Fixed parameters: d = 1000 mm, z_t = 500 mm, σ = 10, t = 20 mm, W = ∞ (100 cycles/mm)

f_c (cycles/mm) =	3	4
Standard tomography		
SNR	0.192	0.211
SNR_a	0.308	0.349
SNR_f	0.508	0.537
Conventional radiology		
SNR	0.186	0.177
SNR_a	0.428	0.460
SNR_f	1.176	0.288
Tomographic filtering		
SNR	0.180	0.124
SNR_a	0.571	0.841
SNR_f	0.262	0.146

the focal spot causes an increase in size of the system impulse response and moving the object (or the plane of cut) closer to the focal spot also causes an increases in the extent of the impulse response. Consequently, an increase of the impulse response size causes an increase of SNR in standard tomography and a decrease of SNR in conventional radiology and tomographic filtering, where SNR_a increases but SNR_f decreases, resulting in a decrease of SNR. These results are in agreement with the conclusions drawn from the practical results in [2], where the difficulty of filtering for layers closer to the focal spot was recognized. One might be tempted to conclude here that a smaller focal spot would be preferred for tomographic filtering. Although this may be true with respect to noise in the image, it is important to recognize that the "noise" due to the presence of other layers is highly structured and not white noise as assumed here. Consequently, larger focal spots may still be preferred [recall (16)]. Since in practice the focal spot is given, the best results will be obtained by adjusting the filter parameters.

Similar results are obtained with variations of the bandwidth of the object (Table IV) or the bandwidth of the low-pass filter (Table V). In standard tomography the SNR increases when the object bandwidth or the cutoff frequency increases. On the other hand, in conventional radiology and tomographic filtering the SNR decreases because it is dominated by SNR_f, which decreases. Note also that when the object is band-limited white noise (i.e., when the cutoff frequency f_c has no effect) in standard tomography SNR_a is equal to SNR_f.

When the system parameters are the same (that is, any column in Tables I to V) the signal-to-noise ratios compare as follows (the arrows denote how they increase):

	SNR_a	SNR_f	SNR
Standard tomography	↓	↑	↑
Conventional radiology			
Tomographic filtering			

Therefore, the SNR is largest for standard tomography and smallest for tomographic filters. From this we should not conclude that tomographic filters are useless because with real objects the noise is structured and the SNR may be perceived differently by the eye. On the other hand, SNR_a is always largest for tomographic filters, which shows that the tomographic filtering technique performs better for layers of the object closer to the film.

E. The Radiation Dose

The goal in diagnostic radiology is to obtain as much relevant information as possible from inside a patient's body, while keeping the total radiation dose to a minimum to reduce any possible danger to the patient.

Each radiologic procedure represents a compromise between dose, and image and diagnostic qualities [9]. Standard tomography must be regarded as a relatively high exposure-dose procedure and it is used only when there are specific indications which outweigh the risks [5, p. 314]. The radiation dose per exposure, typically 1-2 rad, is comparable to conventional radiology, but the total dose is usually greater since multiple exposures are the rule. Indeed, since the location of the relevant structures is not usually known, various tomograms have to be obtained until their positions are known; this is especially true in the case that the details are small. It was formerly believed that the dose in standard tomography could be kept low using a simultaneous multisection technique. Instead of using just one film, several films (typically five or six) are contained in a multicassette box and spaced at about 1 cm apart. However, the total dose to the patient is not reduced if intensifying screens are used, in which case the patient dose is comparable to the one with the same number of single section exposures [10].

Here the advantage of a tomographic filtration process is clear. With a single radiograph and tomographic filtering operations an indication of the positions of the structures can be obtained. Once they are known, a subsequent thin-section tomogram at the proper depth using standard techniques may give a more accurate representation. Indeed, it has been suggested [9] that a diagnostic hierarchy could be formulated which would significantly reduce the total radiation levels to which specific types of patients are exposed. A tomographic filtration process would fit well in such a hierarchy, especially when on-line image processing and communication systems [11] are available in hospitals which will facilitate the storage, retrieval, processing, and display of the images.

IV. Practical Evaluations of Tomographic Filters

Practical evaluations of tomographic filters were also carried out [2]. Examples of results with computer simulated radiographs were published in [12]. Here, some results with actual radiographs are shown and discussed. Radiographs of a mock chest (phantom) with different sets of lesions on either side of the chest were obtained at the Radiological Research Laboratories, University of Toronto, Canada. In order to have sufficient resolution, only small areas of 50×50 mm^2 in the radiograph were digitized. Fig. 3 shows two examples obtained with a focal spot of nominal size 2 mm, and radiological magnifications of 1.5X [Fig. 3(a)] and 2X [Fig. 3(b)]. The regions to be processed were carefully chosen to contain two lesions, one on the side of the chest closest to the focal spot (small white area in the fourth quadrant) and one on the side of the chest closest to the film (large white area in the second quadrant). We will refer to these two layers as layer 2 and layer 1, respectively.

The number of samples in the processed radiographs was 140×140 and in the filter impulse responses 117×117 (separable). The parameters of the tomographic filters used are given in Table VI. The need for, and definition of, hard limits and cutoff frequencies, as well as further details on the filter design and implementation techniques, can be found in [2], [12].

The results are shown in Figs. 4 and 5. In general, the reconstruction of the layer of the phantom which is closest to the focal spot (layer 2) produces a sharper image of the lesion in that layer and also an apparent reduction of its size [see fourth quadrant in Fig. 4(a) and (b) and Fig. 5(a) and (b)]. The same

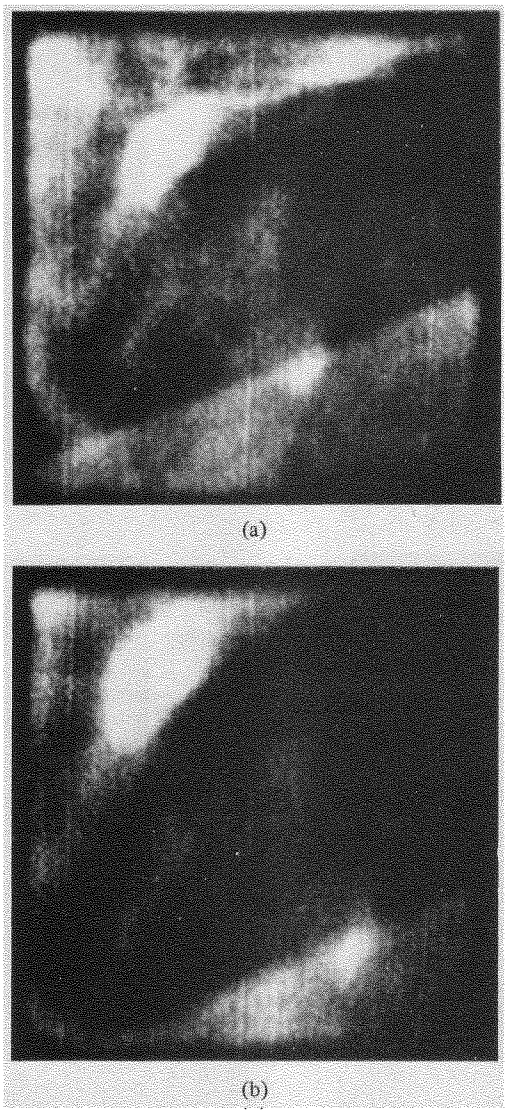

Fig. 3. Two digitized, windowed, and reconstructed radiographs of the same object. Radiological magnification: (a) 1.5× (b) 2×.

TABLE VI
SUMMARY OF THE PARAMETERS OF THE TOMOGRAPHIC FILTERS USED TO OBTAIN FIGS. 4 AND 5

RESULTING FIGURE	ORIGINAL FIGURE	LAYER TO DEBLUR	HARD LIMIT (in dB)	LOW-PASS FILTER BANDWIDTHS (in cycles/mm) f_{c_1}	f_{c_2}
4(a)	3(a)	2	10	0.34	0.37
4(b)	3(a)	2	20	0.41	0.51
4(c)	3(a)	1	15	1.32	0.94
4(d)	3(a)	1	20	1.48	1.11
5(a)	3(b)	2	20	0.24	0.30
5(b)	3(b)	2	20	0.70	0.30
5(c)	3(b)	1	10	1.07	0.39
5(d)	3(b)	1	20	0.40	0.53

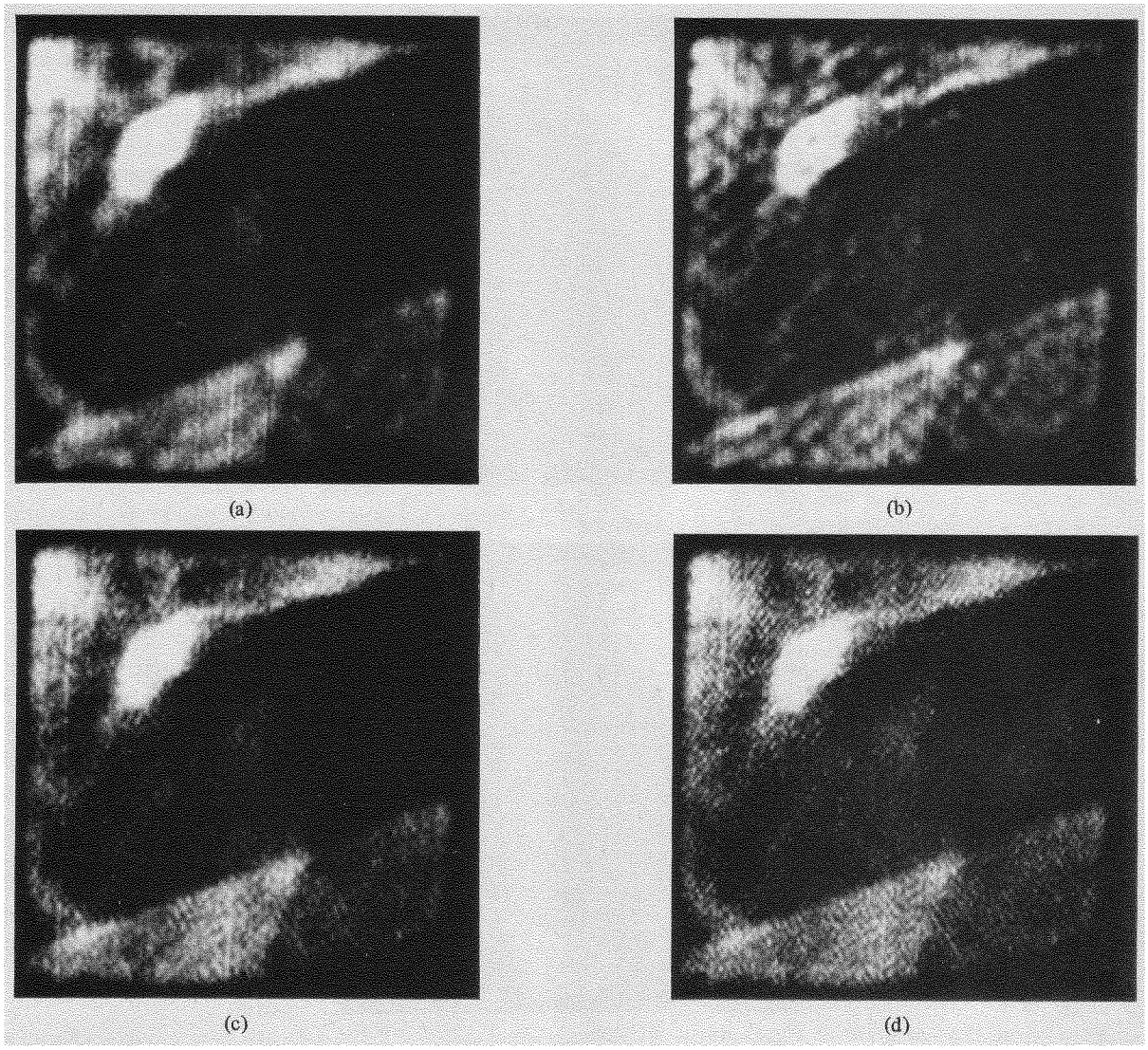

Fig. 4. (a)-(d) Results of filtering Fig. 3(a) with tomographic filters. The parameters are given in Table VI.

filter degrades the large lesion in the layer of the phantom closest to the film (layer 1), by filling it with gray levels [see second quadrant in Fig. 4(a) and (b) and Fig. 5(a) and (b)]. On the other hand, the reconstruction of layer 1 degrades the image of the lesion on layer 2 by smearing it in the background [see fourth quadrant in Fig. 4(c) and (d) and Fig. 5(c) and (d)].

V. Conclusions

Tomographic filtering is a new technique that filters conventional radiographs for the simulation of standard tomography. Tomographic filters could easily be applied when on-line image processing and communication systems are available in hospitals, thus facilitating the storage, retrieval, processing, and display of the images. This paper has produced a comparative assessment of tomographic filtering with respect to standard tomography and conventional radiology. Practical evaluations have also been shown.

In terms of the exposure angle, a tomographic filtration process is closer to zonography than to any other tomographic technique. When exposure angle is translated to thickness of cut, the result gives a clear advantage to standard tomography over tomographic filtering, but tomographic filtering represents an improvement over conventional radiography.

The magnitude transfer function in a TFP varies faster from layer to layer than in the equivalent system using standard tomography. It has been shown that this interval always contains the plane of cut, hence, in a region around the tomographic layer a TFP gives better contrast between layers than standard tomography. However, if the normal sizes of the exposure function are taken into consideration, the performance of standard tomography is by far better because that interval becomes negligible.

The signal-to-noise ratio is another useful evaluation criterion which has served to compare the characteristics of the three techniques. Nevertheless, these measures give only an indication of the performance from a theoretical point of view. In practice, the object is very structured and the effects of noise cannot be calculated statistically.

The greatest advantage of a tomographic filtration process is in reducing the radiation dose to the patient. Indeed, a single radiograph and tomographic filtering operations might give

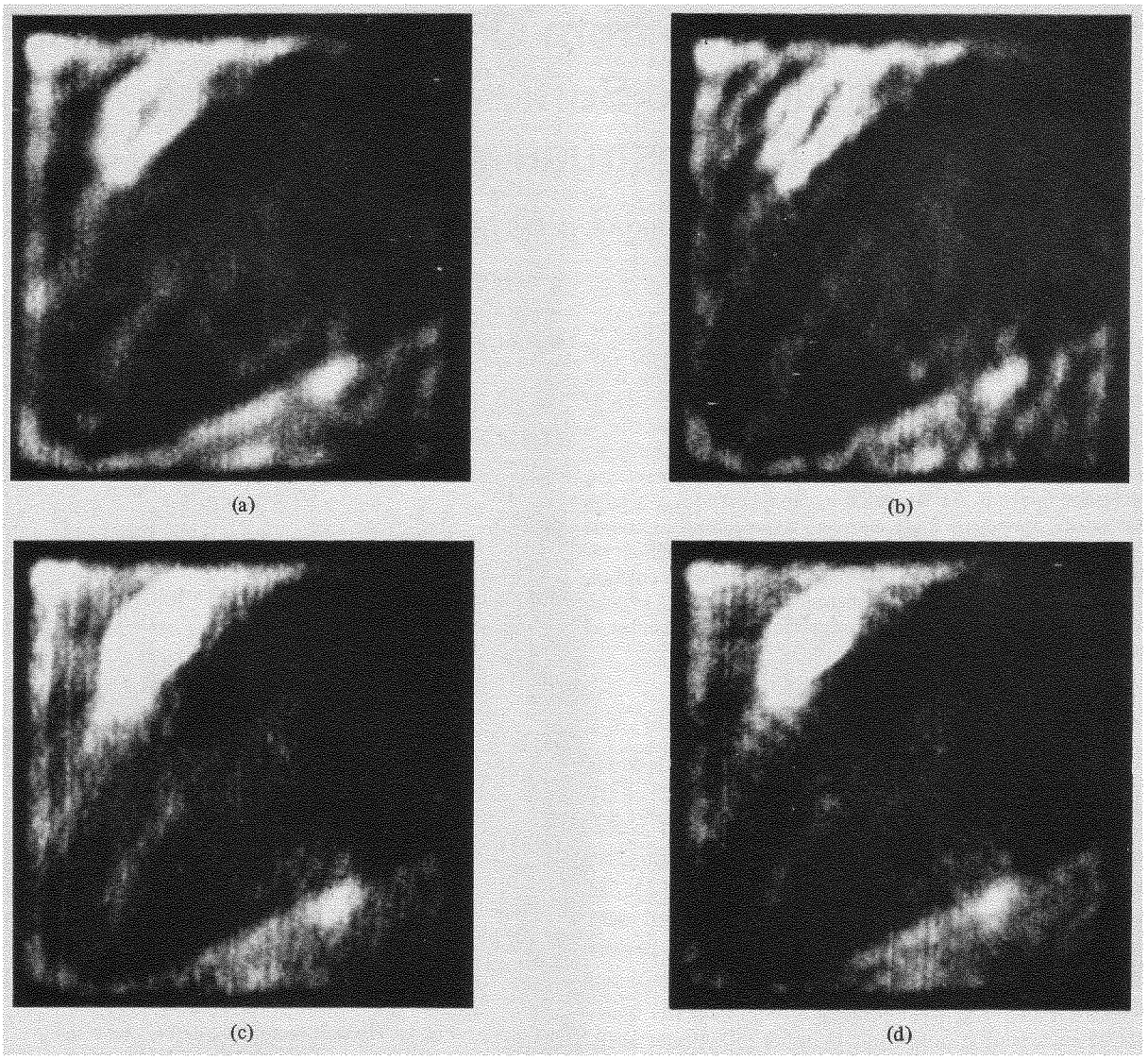

Fig. 5. (a)–(d) Results of filtering Fig. 3(b) with tomographic filters. The parameters are given in Table VI.

enough depth information. If more details are needed, a subsequent thin-section tomogram would give a more accurate representation at the proper depth, without multiple exposures.

Further research is required to determine those medical procedures that would benefit more from tomographic filters. Specific suggestions were given in [12].

REFERENCES

[1] J. M. Costa, A. N. Venetsanopoulos, and M. Trefler, "Digital tomographic filtering of radiographs," *IEEE Trans. Med. Imaging*, vol. MI-2, pp. 76–88, June 1983.

[2] J. M. Costa, "Design and realization of tomographic filters for radiographs," Ph.D. dissertation, Univ. Toronto, Ont., Canada, 1982.

[3] —, "Tomographic filters for digital radiography," in *Digital Radiography, Proc. Soc. Photo-Opt. Instrum. Eng.*, vol. 314, pp. 64–71, 1981.

[4] W. J. Meredith and J. B. Massey, *Fundamental Physics of Radiology*, 2nd ed. Bristol, England: J. Wright, 1972.

[5] A. Berrett, S. Brünner, and G. E. Valvassory, Eds., *Modern Thin-Section Tomography*. Springfield, IL: Charles C Thomas, 1973.

[6] D. Westra, "Zonography. The narrow-angle tomography," thesis, Excerpta Medica Foundation, Amsterdam, The Netherlands, 1966.

[7] K. Lindblom, "On microtomography," *Acta Radiologica (Stockholm)*, vol. 42, p. 465, 1954.

[8] S. C. Orphanoudakis and J. W. Strohbehn, "Mathematical model of conventional tomography," *Med. Phys.*, vol. 3, pp. 224–232, July/Aug. 1976.

[9] W. Maue-Dickson and M. Trefler, "Image quality in computerized and conventional tomography in the assessment of craniofacial anomalies," Univ. Miami School Medicine, Miami, FL, Aug. 26, 1977.

[10] B. C. Ziedses des Plantes, "Relative patient dose in conventional radiology, tomography, multisection radiography, and radiographic subtraction," in *The Reduction of Patient Dose by Diagnostic Radiologic Instrumentation*, R. D. Moseley and J. H. Rust, Eds. Springfield, IL: Charles C Thomas, 1964, p. 71.

[11] J. M. Costa, "Medical image communication systems," in *Digital Radiography, Proc. Soc. Photo-Opt. Instrum. Eng.*, vol. 314, pp. 380–388, 1981.

[12] J. M. Costa, A. N. Venetsanopoulos, and M. Trefler, "Design and implementation of digital tomographic filters," *IEEE Trans. Med. Imaging*, vol. MI-2, pp. 89–100, June 1983.